REPORT DOCUMENTATION PAGE

Form Approved OMB NO. 0704-0188

1. REPORT DATE (DD-MM-YYYY)	2. REPORT TYPE	3. DATES COVERED (From - To)
25-09-2014	Final Report	1-Apr-2011 - 30-Jun-2014

4. TITLE AND SUBTITLE
Final Report: Novel Design of Type I High Power Mid-IR Diode Lasers for Spectral Region 3 - 4.2 Microns.

5a. CONTRACT NUMBER
W911NF-11-1-0109

5b. GRANT NUMBER

5c. PROGRAM ELEMENT NUMBER
611102

6. AUTHORS
Leon Shterengas, Gregory Belenky, David Westerfeld

5d. PROJECT NUMBER

5e. TASK NUMBER

5f. WORK UNIT NUMBER

7. PERFORMING ORGANIZATION NAMES AND ADDRESSES
Research Foundation of SUNY at Stony Brc
W-5510 Melville Library

West Sayville, NY 11796 -3362

8. PERFORMING ORGANIZATION REPORT NUMBER

9. SPONSORING/MONITORING AGENCY NAME(S) AND ADDRESS (ES)
U.S. Army Research Office
P.O. Box 12211
Research Triangle Park, NC 27709-2211

10. SPONSOR/MONITOR'S ACRONYM(S)
ARO

11. SPONSOR/MONITOR'S REPORT NUMBER(S)
57965-EL.15

12. DISTRIBUTION AVAILIBILITY STATEMENT
Approved for Public Release; Distribution Unlimited

13. SUPPLEMENTARY NOTES
The views, opinions and/or findings contained in this report are those of the author(s) and should not contrued as an official Department of the Army position, policy or decision, unless so designated by other documentation.

14. ABSTRACT
Novel designs of the mid-infrared GaSb-based diode lasers were studied including those based on triple layer quantum well active regions, metamorphic virtual substrate and cascade pumping scheme. Cascade pumping of type-I quantum well gain section opened the whole new avenue of the mid-infrared diode laser development with the prospect of multifold improvement of the device characteristics. Cascade pumping was achieved utilizing efficient interband tunneling through "leaky" window in band alignment at GaSb/InAs heterointerface. The 100% efficient carrier recycling between stages was confirmed by twofold increase light-current characteristics slope of

15. SUBJECT TERMS
mid-infrared diode lasers, antimonide diode lasers, metamorphic lasers, cascade diode lasers, high power

16. SECURITY CLASSIFICATION OF:			17. LIMITATION OF ABSTRACT	15. NUMBER OF PAGES	19a. NAME OF RESPONSIBLE PERSON
a. REPORT	b. ABSTRACT	c. THIS PAGE			Gregory Belenky
UU	UU	UU	UU		19b. TELEPHONE NUMBER 631-632-8397

Report Title

Final Report: Novel Design of Type I High Power Mid-IR Diode Lasers for Spectral Region 3 - 4.2 Microns.

ABSTRACT

Novel designs of the mid-infrared GaSb-based diode lasers were studied including those based on triple layer quantum well active regions, metamorphic virtual substrate and cascade pumping scheme. Cascade pumping of type-I quantum well gain section opened the whole new avenue of the mid-infrared diode laser development with the prospect of multifold improvement of the device characteristics. Cascade pumping was achieved utilizing efficient interband tunneling through "leaky" window in band alignment at GaSb/InAs heterointerface. The 100% efficient carrier recycling between stages was confirmed by twofold increase light-current characteristics slope of two-stage 2.4 – 3.3 μm cascade lasers as compared to reference single-stage devices. The cascade pumping scheme reduced threshold current density of high power type-I quantum well GaSb-based ? ~ 3 μm diode lasers down to ~100 A/cm2 at room temperature. Devices with densely stacked two and three gain stages and 100-μm-wide aperture demonstrated peak power conversion efficiency of 16% and continuous wave output power of 960 mW. Corresponding narrow ridge lasers demonstrated above 100 mW of output power. Devices

Enter List of papers submitted or published that acknowledge ARO support from the start of the project to the date of this printing. List the papers, including journal references, in the following categories:

(a) Papers published in peer-reviewed journals (N/A for none)

Received		Paper
09/10/2012	1.00	T Hosoda, D Wang, G Kipshidze, W L Sarney, L Shterengas, G Belenky. 3 μm diode lasers grown on (Al) GaInSb compositionally graded metamorphic buffer layers, Semiconductor Science and Technology, (05 2012): 55011. doi: 10.1088/0268-1242/27/5/055011
09/10/2012	4.00	G. Belenky, D. Donetsky, G. Kipshidze, D. Wang, L. Shterengas, W. L. Sarney, S. P. Svensson. Properties of unrelaxed InAs1?XSbX alloys grown on compositionally graded buffers, Applied Physics Letters, (10 2011): 141116. doi: 10.1063/1.3650473
09/10/2012	2.00	S. P. Svensson, H. Hier, W. L. Sarney, G. Kipshidze, D. Donetsky, D. Wang, L. Shterengas, G. Belenky. Structural and luminescent properties of bulk InAsSb, Journal of Vacuum Science & Technology B: Microelectronics and Nanometer Structures, (02 2012): 105. doi: 10.1116/1.3670749
09/11/2013	5.00	Leon Shterengas, Gregory Belenky, Wendy Sarney, Stefan Svensson, Ding Wang, Dmitry Donetsky, Gela Kipshidze, Youxi Lin. Metamorphic InAsSb-based barrier photodetectors for the long wave infrared region, Applied Physics Letters, (08 2013): 51120. doi: 10.1063/1.4817823
09/11/2013	6.00	Leon Shterengas, David Westerfeld, Wendy L. Sarney, Stefan P. Svensson, Gregory Belenky, Ding Wang, Youxi Lin, Dmitry Donetsky, Gela Kipshidze. Metamorphic InAsSb/AlInAsSb heterostructures for optoelectronic applications, Applied Physics Letters, (05 2013): 111108. doi: 10.1063/1.4796181
09/11/2013	7.00	W. L. Sarney, H. Hier, Y. Lin, D. Wang, S. P. Svensson, D. Donetsky, L. Shterengas, G. Kipshidze, G. Belenky. Band gap of InAs_{1?x}Sb_{x} with native lattice constant, Physical Review B, (12 2012): 245205. doi: 10.1103/PhysRevB.86.245205
09/25/2014	11.00	Rui Liang, Gela Kipshidze, Takashi Hosoda, Leon Shterengas, Gregory Belenky. 3.3-3.4-um Diode Lasers Based on Triple-Layer GaInAsSb Quantum Wells, IEEE Photonics Technology Letters, (04 2014): 0. doi: 10.1109/LPT.2014.2302835
10/15/2013	9.00	Leon Shterengas, Rui Liang, Gela Kipshidze, Takashi Hosoda, Sergey Suchalkin, Gregory Belenky. Type-I quantum well cascade diode lasers emitting near 3??m, Applied Physics Letters, (08 2013): 121108. doi: 10.1063/1.4821992
TOTAL:		**8**

Number of Papers published in peer-reviewed journals:

(b) Papers published in non-peer-reviewed journals (N/A for none)

Received Paper

TOTAL:

Number of Papers published in non peer-reviewed journals:

(c) Presentations

Number of Presentations: 0.00

Non Peer-Reviewed Conference Proceeding publications (other than abstracts):

Received Paper

TOTAL:

Number of Non Peer-Reviewed Conference Proceeding publications (other than abstracts):

Peer-Reviewed Conference Proceeding publications (other than abstracts):

Received		Paper
09/11/2013	8.00	Ding Wang, Youxi Lin, Dmitry Donetsky, Gela Kipshidze, Leon Shterengas, Gregory Belenky, Stefan P. Svensson, Wendy L. Sarney, Harry Hier, Bjørn F. Andresen, Gabor F. Fulop, Charles M. Hanson, Paul R. Norton, Patrick Robert. Infrared emitters and photodetectors with InAsSb bulk active region, SPIE Defense, Security, and Sensing. 29-APR-13, Baltimore, Maryland, USA. : ,
09/25/2014	10.00	L. Shterengas, R. Liang, G. Kipshidze, T. Hosoda, S. Suchalkin, G. Belenky. Cascade pumping of GaSb-based type-I quantum well diode lasers, SPIE OPTO. 01-FEB-14, San Francisco, California, United States. : ,
09/25/2014	13.00	Rui Liang, Leon Shterengas, Takashi Hosoda, Aaron Stein, Ming Lu, Gela Kipshidze, Gregory Belenky. Diffraction limited 3.15 μm cascade diode lasers, 2014 72nd Annual Device Research Conference (DRC). 22-JUN-14, Santa Barbara, CA, USA. : ,
TOTAL:		**3**

Number of Peer-Reviewed Conference Proceeding publications (other than abstracts):

(d) Manuscripts

Received		Paper
09/25/2014	12.00	Youxi Lin, Ding Wang, Dmitry Donetsky, Gela Kipshidze, Leon Shterengas, Gregory Belenky, Wendy L. Sarney, Stefan P. Svensson. Structural and Optical Characteristics of Metamorphic Bulk InAsSb, International Journal of High Speed Electronics and Systems (03 2014)
09/25/2014	14.00	Rui Liang, Leon Shterengas, Takashi Hosoda, Aaron Stein, Ming Lu, Gela Kipshidze, Gregory Belenky. Diffraction Limited 3.15 μm Cascade Diode Lasers, Semiconductor Science and Technology (07 2014)
TOTAL:		**2**

Number of Manuscripts:

Books

Received Book

TOTAL:

Received Book Chapter

TOTAL:

Patents Submitted

Patents Awarded

Awards

Graduate Students

NAME	PERCENT_SUPPORTED	Discipline
Rui Liang	0.05	
Youxi Lin	0.05	
FTE Equivalent:	**0.10**	
Total Number:	**2**	

Names of Post Doctorates

NAME	PERCENT_SUPPORTED
Takashi Hosoda	0.05
Gela Kipshidze	0.05
Sergey Suchalkin	0.09
FTE Equivalent:	**0.19**
Total Number:	**3**

Names of Faculty Supported

NAME	PERCENT_SUPPORTED	National Academy Member
Leon Shterengas	0.08	
Dmitri Donetski	0.08	
FTE Equivalent:	**0.16**	
Total Number:	**2**	

Names of Under Graduate students supported

NAME	PERCENT_SUPPORTED
FTE Equivalent:	
Total Number:	

Student Metrics

This section only applies to graduating undergraduates supported by this agreement in this reporting period

The number of undergraduates funded by this agreement who graduated during this period: 0.00

The number of undergraduates funded by this agreement who graduated during this period with a degree in science, mathematics, engineering, or technology fields:..... 0.00

The number of undergraduates funded by your agreement who graduated during this period and will continue to pursue a graduate or Ph.D. degree in science, mathematics, engineering, or technology fields:..... 0.00

Number of graduating undergraduates who achieved a 3.5 GPA to 4.0 (4.0 max scale):..... 0.00

Number of graduating undergraduates funded by a DoD funded Center of Excellence grant for Education, Research and Engineering:..... 0.00

The number of undergraduates funded by your agreement who graduated during this period and intend to work for the Department of Defense 0.00

The number of undergraduates funded by your agreement who graduated during this period and will receive scholarships or fellowships for further studies in science, mathematics, engineering or technology fields: 0.00

Names of Personnel receiving masters degrees

NAME
Total Number:

Names of personnel receiving PHDs

NAME
Total Number:

Names of other research staff

NAME	PERCENT_SUPPORTED

FTE Equivalent:
Total Number:

Sub Contractors (DD882)

Inventions (DD882)

Scientific Progress

The cascade pumping scheme reduced threshold current density of high power type-I quantum well GaSb-based ? ~ 3 μm diode lasers down to ~100 A/cm2 at room temperature. Laser heterostructures had single GaInAsSb quantum well gain stages connected in series by means of GaSb/AlSb/InAs tunnel junctions followed by InAs/AlSb electron injectors. Devices with densely stacked two and three gain stages and 100-μm-wide aperture demonstrated peak power conversion efficiency of 16% and continuous wave output power of 960 mW. Corresponding narrow ridge lasers demonstrated above 100 mW of output power. The experiment showed that the bandwidth of the gain and its rate of increase with current depended strongly on the thickness of AlSb layer separating electron injectors from quantum wells. The possible impact of electron injector interfaces and ionized impurities on the carrier scattering and recombination in the active quantum well is discussed.

"See Attachment"

Technology Transfer

Cascade type-I quantum well diode lasers emitting 960 mW near 3 μm.

Cascade pumping design scheme can address fundamental challenges associated with mid-infrared diode laser heterostructures. It offers efficient means to minimize the quantum well (QW) threshold carrier concentration and the corresponding adverse effect of Auger recombination. Threshold carrier concentration is reduced through improvement of the optical confinement factor by connecting multiple gain stages in series without dealing with usual issues* encountered by merely increasing the number of QWs within standard diode laser active regions. Possibility to minimize threshold current while simultaneously increasing device internal efficiency makes cascade pumping an enabling design solution for high power efficient lasers emitting near and above 3 μm.

Initially cascade pumping scheme was applied to laser heterostructures utilizing gain sections based on either intersubband [1] or type-II interband [2] electron transitions, see for instance [3,4,5]. We have shown [6] that, at least within antimonide material system, the cascade pumping scheme is compatible with type-I QW interband gain sections providing efficient carrier recycling between stages leading to internal efficiencies in excess of 100% . Corresponding high power room temperature operated 2.4 – 3.3 μm two-stage cascade diode lasers were fabricated [7]. Experiment confirmed that interband tunnel junction followed by electron injector located near anti-node of the laser mode did not lead to excessive internal optical loss. In devices reported previously [6] the separation between active QW and electron injector was above 200 nm (see structure R in Figure 1). Large spacing eliminated any interaction between gain section and injector but led to reduced QW optical confinement factor. Consequently a potential of the cascade pumping scheme to minimize threshold current density and improve power-conversion efficiency was not fully realized.

In this work we eliminated the separations between the active quantum well and the electron injector (see structures A & B in Figure 1). This design was implemented in order to reduce threshold current density and improve device efficiency. New generation of $\lambda \sim 3$ μm cascade diode lasers demonstrated CW RT threshold current densities as low as 100 A/cm^2. Peak CW RT power conversion efficiency was ~16% for two-stage 2-mm-long 100-μm-wide ridge coated lasers. Corresponding narrow ~6-μm-wide ridge lasers generated above 100 mW in nearly diffraction limited beam. Three stage 3-mm-long wide ridge coated lasers demonstrated CW output power level of960 mW at 17 ^{0}C.

Figure 1 shows band diagram schematics of the laser heterostructures studied. Each was grown by solid-source molecular beam epitaxy on GaSb substrates with the following common characteristics. The n- and p-cladding layers were made of $Al_{80}Ga_{20}As_7Sb_{93}$ doped with Te and Be, respectively. The barrier and waveguide core layers were nominally undoped $Al_{20}Ga_{55}In_{25}As_{23}Sb_{77}$ [8]. Compressively strained (~1.5%)12 nm-wide GaInAsSb layers, with ~50% Indium, comprised the QWs responsible for the room temperature optical gain near 3 μm. Graded layer was nominally undoped AlGaAsSb with Al composition changing from 50% down to ~5% over thickness of 100-nm. The graded layer was followed by tunnel junction and electron

*Among those are buildup of the transparency current and development of pumping inhomogeneity across multiple-QW section often accompanied by injection efficiency degradation.

injector comprised of nominally undoped 10-nm-thick GaSb, 2.5-nm-thick AlSb and Te-doped 6-period InAs/AlSb chirped superlattice (SL).The grown structures were processed into 100-μm-wide and ~6-μm-wide dielectric confined ridge lasers.

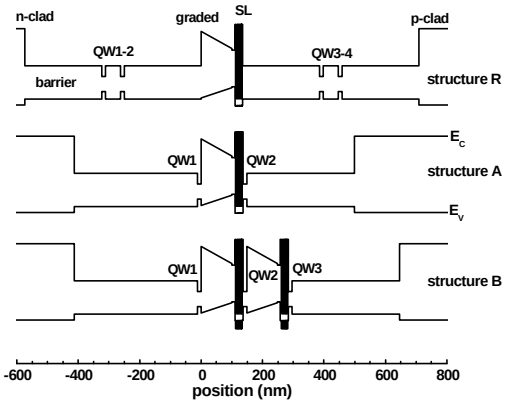

Figure 1. Schematic band diagram of the laser heterostructures under flat band condition.

Structure R (Figure 1) depicts the design of the first reported type-I QW GaSb-based diode laser [6], and used in this work as a baseline reference sample. It was designed so that the fundamental optical mode overlapped the two double-QW narrow waveguide laser active regions separated by a tunnel junction and electron injector with 1.2-nm-thick AlSb layers. This two-stage cascade laser design exhibited a slope efficiency twice that reported for standard single stage type-I QW GaSb-based diode laser heterostructures [9]. Note however, that neither the differential gain nor the threshold current density of the cascade lasers utilizing Structure R improved because of a nearly twofold reduction of the optical confinement factor per QW.

Structure A shown in Figure 1 was developed specifically to increase the optical confinement factor of active QWs and to minimize threshold current density. To accomplish this, the QWs were moved close to the anti-node of the fundamental waveguide optical mode and, thus, located adjacent to the graded and electron injector layers. Also, the number of QWs in each cascade was reduced to one. It was expected that Structure A would reduce the threshold current density by a factor of 2, double the slope efficiency, and thereby enhance the power conversion efficiency (PCE).

The PCE can be written using a piecewise model of current-voltage characteristics as:

$$PCE(I) = \frac{\eta \cdot (I - I_{TH})}{I \cdot (V_0 + I \cdot R_S)}, \qquad (1)$$

where η is the device slope efficiency, I is the current, I_{TH} is the threshold current, V_0 is the voltage drop across active region, and R_S is series resistance. The peak PCE can be estimated by differentiating Eq. 1(and ignoring the effects of Joule heating):

$$PCE_{MAX} = \frac{\eta}{I_{TH} \cdot R_S} \cdot \left(1 + \sqrt{1 + \frac{V_0}{I_{TH} \cdot R_S}}\right)^{-2}. \qquad (2)$$

Clearly, both reduction of the threshold current and increase of the slope efficiency are beneficial, but the latter has a more pronounced effect.

The three-stage cascade diode laser design (Structure B in Figure 1) resulted from adding an extra single-QW gain stage to Structure A. It was expected that the efficiency, threshold current, and voltage drop across active region would scale with number of gain stages. However, our results indicated that the extent of this scaling depended heavily on the interaction between the QWs and adjacent electron injectors.

Figure 2a shows room temperature plots of Hakki-Paoli modal gain spectra [10] acquired from 100-μm-wide 1-mm-long uncoated lasers based on structures R and A.

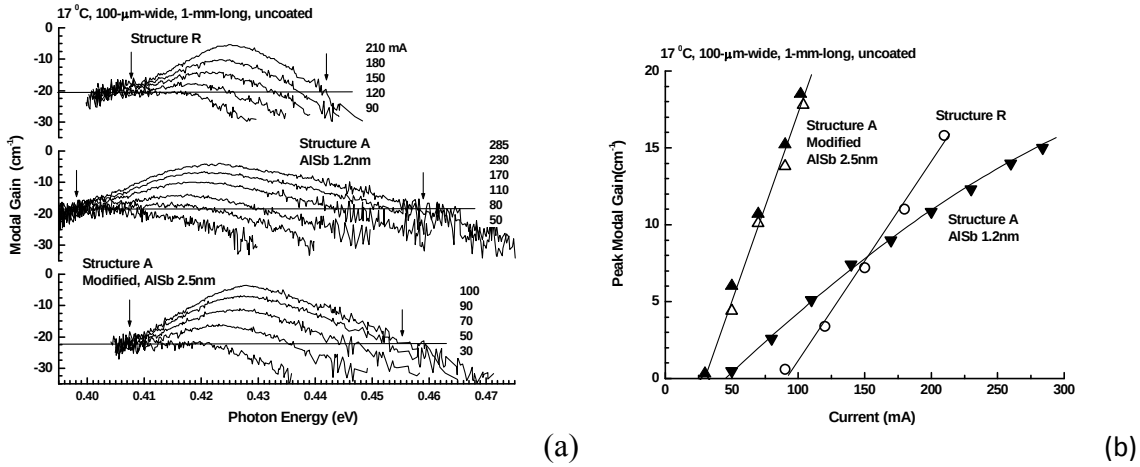

Figure 2.
(a) Modal gain spectra measured by Hakki-Paoli method for two-stage cascade lasers based on structure R, A and modified A. The measurement was done at 17 ^{0}C for 1-mm-long, 100-μm-wide uncoated lasers in pulsed regime;
(b) Current dependences of the peak modal gain of lasers based on structure R (open circles), structure A (solid down triangles), modified structure A (solid upward triangles), modified structure A with undoped last 4 periods of SL (open upward triangles).

They all had net cavity losses (horizontal solid lines in Figure 2a) between 20 and 22 cm^{-1}, which corresponded to internal optical losses of 8 - 10 cm^{-1}.The bandwidth of the gain spectra(measured at the locations of the estimated cavity loss level indicated by the vertical arrows shown in Figure 2a) was less than 40 meV near threshold for the devices based on structure R. This gain bandwidth was comparable to that typically measured for standard GaSb-based type-I QW diode lasers emitting near and above 3 μm [9].The latter observation is predictable since two-stage cascade lasers based on structure R utilize the same symmetric QWs as standard diode lasers do. In structure A the QWs have asymmetric barriers and QW2 (Figure 1) is grown directly on top of the last AlSb layer of chirped InAs/AlSb SL electron injector. The nominal thickness of all AlSb layers in electron injector of both structure R and A was 1.2 nm. Devices based on structure A demonstrated nearly twofold increase in threshold gain bandwidth (middle plot in Figure 2a). Gain broadening was accompanied by severe suppression of differential gain with respect to current (close downward triangles in Figure 2b) leading to threshold current degradation. In modified version of structure A the thickness of only the last (directly preceding QW2) AlSb layer of electron injector was increased from 1.2 to 2.5 nm. This modification of structure A design resulted in a diminished gain bandwidth (bottom plot in Figure 2a) and significantly improved differential gain with respect to concentration (close upward triangles in Figure 2b). It was notable that eliminating the Te doping from

the last four layers of InAs/AlSb SL of the modified structure A did not lead to further improvements of the modal gain (e.g., compare open to close triangle of Fig. 2b) or the gain bandwidth. This suggested that the gain broadening observed for lasers based on structure A (Figure 2a) could be attributed to enhanced effect of surface roughness scattering [11]in QW2 associated with a the narrow AlSb barrier. This contention was further corroborated by previously performed independent experiments that demonstrated that replacing the right barrier of QW1 with graded layer while keeping QW2 barriers symmetric like in Structure R had only minor effects on gain bandwidth.

One can speculate that penetration of the electron envelope function associated with QW2 into InAs/AlSb SL leads to a decreased intrasubband dephasing time. Presumably, surface roughness scattering that occurs at the InAs/AlSb heterointerface nearest to QW2 contributes the most to gain broadening[†]. In addition, the increased net wave function overlap with heterointerfaces can lead to increased Auger [12] and other nonradiative recombination rates. Therefore, we posit that both gain broadening and reduced carrier lifetime contribute to the decrease of the differential gain with respect to current observed in lasers based on not modified Structure A.

Figure 3 shows plots of CW power and power conversion versus current acquired at 17° C from 100-μm×2-mm anti- and high-reflection (AR/HR) coated two-stage lasers based on modified Structure A. The threshold current density was~100 A/cm^2, the maximum power was~650 mW. Power conversion efficiency reached~16% and remained well above 10% for output powersabove~600 mW. All of these characteristics surpassed those of the previous state-of-the-art 3 μm lasers (i.e., reference structure R) [6]. Of particular note was the nearly twofold reduction of the threshold current density and corresponding improvement of the power conversion efficiency predicted by equation (2). The inserts to Figure 3 show the light-current characteristics and far field patterns for narrow ridge lasers fabricated from the same material. Note that the CW output power from this device was above 100 mW.

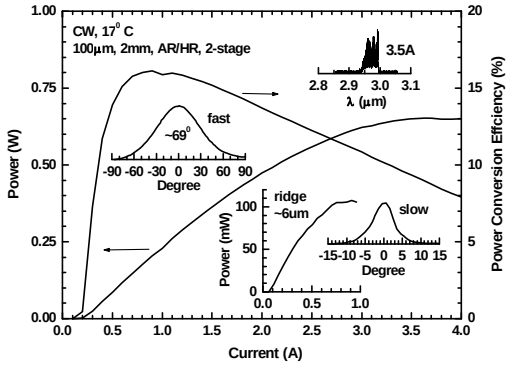

Figure 3. CW light-current-power conversion characteristics measured at 17 ^{0}C for 100-μm-wide, 2-mm-long AR/HR coated two-stage cascade lasers. Inserts show laser spectra at maximum power level, fast axis far field pattern as well as CW light-current characteristics of 2-mm-long, AR/HR coated narrow ridges with corresponding slow axis far field pattern.

[†] Impurity scattering associated with Te ions in doped InAs layers is less probable candidate since increase of the AlSb barrier thickness by just ~1.3 nm in modified structure A led to dramatic improvement of the device differential gain.

Figure 4 shows plots CW light-current-voltage data acquired from (AR/HR) coated lasers fabricated from material grown according to structure B (i.e., three-stage cascade lasers). Data was acquired from a 100-μm×2-mm laser at temperatures between 17° C and 70° C. The design improvements incorporated into structure B increased this device's CW output power to 830 mW 17^0 C. The structure B laser had T_0 and T_1 values above 50 K and above 110 K, respectively, and a 70^0 C maximum output power greater than 100 mW. The output power of 100-μm×3-mm three-stage laser was increased to ~960 mW at 17 ^{0}C thanks to improved thermal footprint. The fast-axis far field beam divergence of three-stage lasers was smaller than that of the two-stage device with narrower waveguide core (compare ~65^0 in Figure 4 versus ~69^0 in Figure 3). Optical gain measurements indicated that the two- and three-stage devices had nearly the same internal optical loss. The internal efficiency of the 100-μm wide three-stage cascade laser was ~190% at room temperature which confirmed the effect of threefold carrier recycling, specifically when compared to the single stage (regular diode devices) having 50% – 60% internal efficiencies [9]. However, the threshold current density for the three-stage lasers was not lower than that of the two-stage devices (compare Figure 3 to Figure 4). We hypothesize that this results from the barrier energy asymmetries pushing the electron envelope wavefunctions in QW2 of Structure B toward the SL side and thereby intensifying adverse interface interactions. At the moment there are insufficient experimental evidence to isolate this fundamental phenomenon from the effects of growth-to-growth variation on carrier localization and lifetimes.

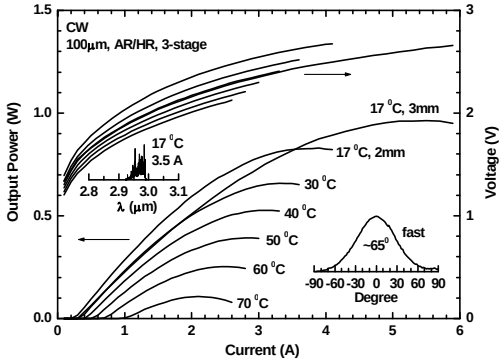

Figure 4. CW light-current-voltage characteristics of 100-μm-wide, 2- and 3-mm-long AR/HR coated three-stage cascade lasers. Inserts shows spectra of the 2-mm-long laser at 17 ^{0}C at maximum output power level and fast axis far field pattern.

In summary, we showed that cascade pumping schemes that utilize single-QW gain stages enhanced both the power conversion efficiency and the output power level of GaSb-based diode lasers that emit near 3 μm at room temperature. The cascade lasers discussed in this work had densely stacked type-I QWs gain stages characterized by high differential gain. The devices demonstrated CW threshold current densities near 100 A/cm^2, a twofold improvement over the previous world record, that resulted in peak power conversion efficiencies increasing to 16% at 17^0C. Three-stage multimode cascade lasers emitted~960 mW of CW output power. Comparable narrow ridge two-stage devices generated more than 100 mW of CW power with ~10% power conversion efficiencies.

References.

1R.F. Kazarinov, R.A. Suris, Fizika i TekhnikaPoluprovodnikov 5: 797 (1971).

2R.Q. Yang, Superlattices and Microstructures 17, 77 (1995).

3 F. Capasso, Optical Engineering 49, 111102 (2010).

4 M. Razeghi, IEEE J. Sel. Top. Quantum Electron.15, 941 (2009).

5 I. Vurgaftman, W.W. Bewley, C.L. Canedy, C.S. Kim, M. Kim, C.D. Merritt, J. Abell, J.R. Meyer, IEEE J. Select. Top.Quantum Electron.19, 1200210 (2013).

6 L. Shterengas, R. Liang, G. Kipshidze, T. Hosoda, S. Suchalkin, G. Belenky, Appl. Phys. Lett., Vol. 103, No. 12, pp. 121108 (2013).

7L Shterengas, R Liang, G Kipshidze, T Hosoda, S Suchalkin, G Belenky, Proc. SPIE OPTO, 900213-10 (2014).

8M. Grau, C. Lin, O. Dier, C. Lauer, M.-C. Amann, Appl. Phys. Lett. 87, 241104 (2005).

9L. Shterengas, G. Kipshidze, T. Hosoda, J. Chen, G. Belenky, Electron, Lett. 45, 942 (2009).

10B. W. Hakki, T. L. Paoli, J. Appl. Phys. 46, 1299 (1975).

11T. Unuma, M. Yoshita, T. Noda, H. Sakaki, H. Akiyama, J. Appl. Phys. 93, 1586 (2003).

12M.I. Dyakonov, V.Yu. Kachorovskii, Phys. Rev. B 49, 17130 (1994).